molecules

MDPI

Article

Synthesis, Structure and Antibacterial Activity of a Neutral Tin(II) Iodide Complex with 1,2-bis[(4-Methoxyphenyl)imino]acenaphthene

Anna A. Tychinina [1,2], Ivan V. Smolyaninov [1], Natalia V. Gogoleva [1], Anton N. Lukoyanov [2,3], Dmitriy S. Yambulatov [1,*] and Mikhail A. Kiskin [1]

[1] Kurnakov Institute of General and Inorganic Chemistry, Russian Academy of Sciences, 31 Leninsky prosp., 119991 Moscow, Russia; anatychinina326@gmail.com (A.A.T.); gogolevanv@inbox.ru (N.V.G.); m_kiskin@mail.ru (M.A.K.)
[2] D. Mendeleev University of Chemical Technology of Russia, 9 Miusskaya Square, 125047 Moscow, Russia
[3] Razuvaev Institute of Organometallic Chemistry, Russian Academy of Sciences, 49 Tropinina Street, 603137 Nizhny Novgorod, Russia
* Correspondence: yambulatov@igic.ras.ru or yambulatov@yandex.ru

Abstract

The reaction of tin(II) iodide with 1,2-bis[(4-methoxyphenyl)imino]acenaphthene (4-MeO-BIAN) in anhydrous tetrahydrofuran afforded the neutral complex [(4-MeO-BIAN)SnI(μ-I)]$_2$ (**1**). A single-phase sample of **1** was isolated and characterized by powder X-ray diffraction and IR spectroscopy. The crystal structure of **1** was determined by single-crystal X-ray diffraction: a centrosymmetric dimeric structure with an Sn_2I_2 core formed by two μ_2-bridging iodide ligands; each Sn(II) center is additionally coordinated by a bidentate 4-MeO-BIAN ligand and one terminal iodide ligand. The antibacterial activity of **1** was evaluated in vitro against clinically significant Gram-positive (*Staphylococcus aureus*, *Enterococcus faecium*, *Enterococcus faecalis*) and Gram-negative (*Escherichia coli*) bacteria. Complex **1** exhibited moderate antibacterial activity against all tested strains, with MIC values of 40–312.5 μg/mL and MBC values of 62.5–312.5 μg/mL. The lowest MIC values, close to those of meropenem (MIC = 32 μg/mL), were obtained against *Staphylococcus aureus* (MIC = 40 μg/mL).

Keywords: tin(II); tin iodide; bis(imino)acenaphthene; redox-active ligands; coordination compounds; X-ray diffraction; antibacterial activity

Check for updates

Academic Editor: Rodica Olar

Received: 3 September 2026
Revised: 11 October 2026
Accepted: 12 October 2026
Published: 14 October 2026

Copyright: © 2026 by the authors. Licensee MDPI, Basel, Switzerland. This article is an open access article distributed under the terms and conditions of the Creative Commons Attribution (CC BY) license.

1. Introduction

Redox-active ligands occupy a special place in modern coordination and bioinorganic chemistry. Unlike "classical" ligands, they are capable of participating in redox processes as well as the central metal atom, reversibly changing their oxidation state and acting as electron reservoirs [1–7]. The redox-active behavior of ligands is widespread in natural systems: molecules such as *o*-quinones, pterins, flavins, and tetrapyrroles function as redox cofactors in the active centers of metalloenzymes containing iron, copper, manganese, and molybdenum [8]. Metal complexes with redox-active ligands are of considerable interest as potential drugs: they can be activated through ligand substitution reactions or redox processes and can simultaneously affect multiple biological targets [9–11]. This ability underlies the high potential of such compounds as antibacterial and antitumor agents [11–13].

Among redox-active ligands, particular attention should be paid to acenaphthene derivatives—bis(arylimino)acenaphthenes (Ar-BIAN) and mono(arylimino)acenaphthenones (Ar-MIAN) [14–16]. Due to the rigid conjugated π-system of the acenaphthene core and two imine groups, these ligands possess high electron affinity and can exist in several oxidation states: neutral, radical-anion, and dianionic [17]. The coordination chemistry of BIAN and MIAN with transition metals is actively developing: complexes of rhodium [18–20], vanadium [21], copper [22], palladium [23,24], and platinum [17] have been obtained and characterized with SC-XRD. Au(I) complexes with BIAN and MIAN ligands also have been structurally characterized by X-ray diffraction, and preliminary biological activity tests have been performed for all complexes [25].

Although tin is not an essential metal, its compounds have long attracted the attention of researchers as potential biologically active agents [26]. Tin complexes exhibit a wide range of pharmacological effects, including antibacterial, antifungal, antioxidant, and anti-tumor activities [26–32]. The coordination of organic ligands to Sn(II) leads to a significant enhancement of the biological effect compared to the free ligands, which is attributed to an increase in the lipophilicity of the complexes and the facilitation of their penetration through microbial cell membranes [33]. Thus, tin(II) complexes represent a promising platform for the development of new biologically active compounds [26,28,34,35].

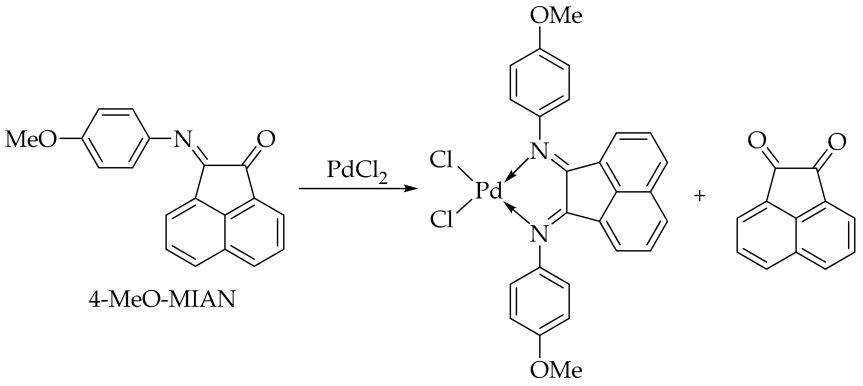
Despite the interest in redox-active acenaphthene derivatives (BIAN, MIAN) and the bioactive properties of tin(II) compounds, their complexes to the best of our knowledge remain poorly studied. The available works on tin with redox-active ligands mainly concern tin(IV) or focus on catalytic and electrochemical properties [36–38]. The aim of this work is the synthesis, structural and electrochemical characterization of the neutral complex [(4-MeO-BIAN)SnI(μ-I)]$_2$, as well as the evaluation of its antibacterial activity. The structure and purity of the obtained compound were characterized by single-crystal and powder X-ray diffraction, IR spectroscopy, and elemental analysis.

2. Results and Discussion

2.1. Synthesis and Characterization of **1**

The reaction of equimolar amounts of tin(II) iodide and the 4-MeO-BIAN ligand in anhydrous THF afforded dark brown crystals of the complex [(4-MeO-BIAN)SnI(μ-I)]$_2$ (**1**) in 84% yield.

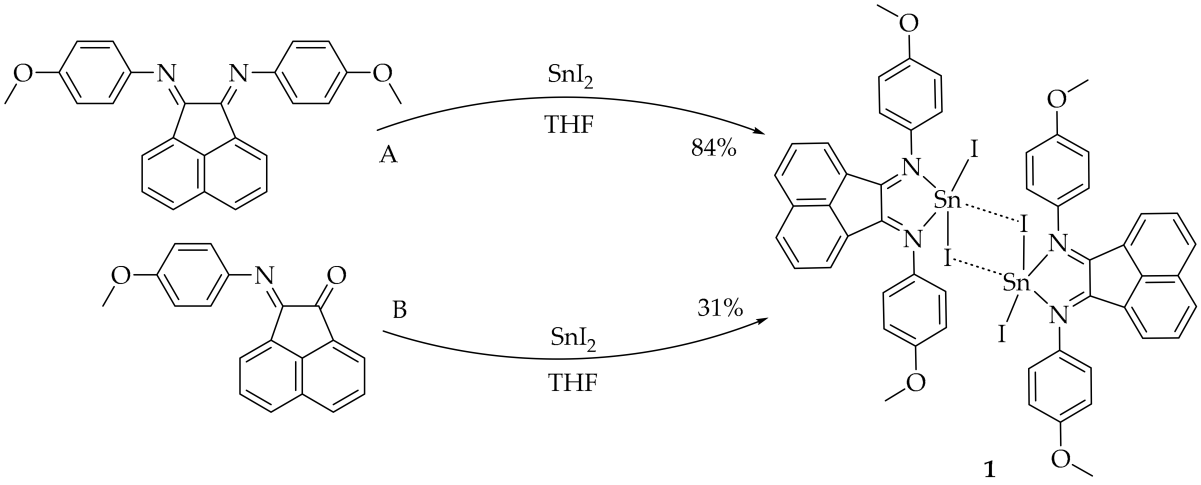
The obtained results demonstrate that the use of 4-MeO-MIAN in the reaction with SnI_2 leads to the formation of the BIAN-containing complex **1**. Similar MIAN-to-BIAN transformations have previously been observed for other metal systems and were attributed to disproportionation of two MIAN molecules with the formation of the corresponding BIAN derivative and acenaphthenequinone: the reaction of $PdCl_2$ with 4-methoxyphenyl-substituted MIAN in dichloromethane is accompanied by a rearrangement of the ligand structure, resulting in the formation of the complex [(4-MeO-BIAN)$PdCl_2$] containing the corresponding BIAN ligand; two MIAN molecules undergo “coupling” to form a diimine BIAN structure in the coordination sphere of the metal (Scheme 1) [21,39]. Our previous studies demonstrated that 4-MeO-MIAN retains its monoiminoacenaphthenone structure upon coordination to a heterometallic Co(II)–Li(I) system [40], whereas its transformation into the corresponding BIAN derivative has been observed for other metal ions [39]. These contrasting coordination behaviors prompted us to investigate the interaction of this particular redox-active ligand system with Sn(II) and to determine whether coordination or ligand rearrangement would occur under these conditions.



Scheme 1. Dimerization of 4-MeO-MIAN into the corresponding BIAN in the reaction with $PdCl_2$.

However, isolation and identification of the organic side products were not the aim of the present study, and acenaphthenequinone was not unambiguously identified in the reaction mixture. Therefore, although the overall ligand transformation appears similar to that reported previously, the available experimental data do not allow us to establish whether it proceeds through exactly the same reaction pathway.

The obtained results indicate that a similar transformation also occurs in the presence of Sn^{2+} ions, leading to the BIAN complex (Scheme 2).



Scheme 2. Synthesis of complex **1**.

At the same time, as was mentioned earlier, when the MIAN ligand (4-MeO-MIAN) was used in the cobalt(II)–lithium(I) complex $[Co_2Li_2(piv)_6(L)_2]$ (piv is an anion of trimethylacetic acid), no rearrangement of the ligand structure was observed, and the MIAN ligand retained its original monoiminoacenaphthenone structure, coordinating through nitrogen and oxygen atoms [40]. Thus, the ability of MIAN ligands to undergo rearrangement depends on the nature of the metal and solvent, the Lewis acidity and the reaction conditions.

The presence of the coordinated 4-MeO-BIAN ligand in **1** was confirmed by IR spectroscopy (see Supplementary Materials, Figure S1). The experimental data confirm the presence of characteristic bands corresponding to C=N stretching vibrations (1697, 1650, 1596, and 1577 cm^{-1}) and C–O–C vibrations of the aromatic ether (1242 and 1018 cm^{-1}). In contrast to complexes containing MIAN ligands, the spectrum of complex **1** does not show the intense band of the carbonyl group C=O stretching vibrations in the region of ~1720 cm^{-1}, which indicates a rearrangement of the ligand structure with the formation of the BIAN derivative, in agreement with the X-ray diffraction data.

2.2. Crystal Structures of **1**

According to single-crystal X-ray diffraction data, complex **1** has a dimeric structure (Figure 1a), in which two tin atoms are symmetrically linked to each other by two μ_2-bridging I2 atoms (Sn–I 3.0908(4), 3.3316(11) Å, I–Sn–I 90.31(3)°, Sn–I–Sn 90.28(16)°; an inversion center is located at the center of the Sn_2I_2 rectangle). The metal atom completes its coordination sphere with two nitrogen atoms of the chelating 4-MeO-BIAN molecule (Sn–N 2.428(3), 2.511(3) Å, N–Sn–N 67.73(11)°) and a terminal iodine atom (Sn–I1 2.9631(4) Å, I1–Sn–I2 93.084(10)°), forming a square pyramid (SnN_2I_3) with the base formed by N2, I1, and two I2 atoms, from the plane of which the tin atom deviates by 0.5591(13) Å, with the apex formed by the N1 atom (τ_5 = 0.02, Figure 1b), or a vacant octahedron (S_Q = 3.760), in which the lone electron pair on the tin atom is directed toward the I1 atom of the neighboring dimer (Sn···I 3.7570(4) Å) with the formation of a supramolecular chain along the 0*a* axis (Figure 1b).

In the coordinated 4-MeO-BIAN molecule, the iminoacenaphthene fragment (C1–N1 1.282(5) Å, C2–N2 1.272(5) Å, C1–C2 1.508(5) Å, $C–C_{range}$ 1.377(7)–1.484(5) Å) is planar, with a root-mean-square deviation of the atoms from the mean plane of 0.061 Å. The phenyl fragments are rotated relative to the BIAN core, with the C–N–C–C dihedral angles being 51.9(6)° and 89.8(5)°. The larger rotation of the aromatic substituent is due to the formation of an intramolecular contact between the hydrogen atom at the 2-position of the phenyl ring and I2 atom (Figure 1a, Table 1). In the crystal, the molecules of the complex additionally interact with each other through non-covalent C–H···O, C–H···I, and C–H···π interactions, forming a three-dimensional network (Table 2).

Table 1. Main parameters of C–H···A contacts in the crystal of complex **1**.

C–H···A	Symmetry Operation	C–H, Å	H···A, Å	C···A, Å	C–H···A, °
C14–H14···I1	–	0.95	3.20	3.957	138
C8–H8···O2	$1+x, -1+y, z$	0.95	2.44	3.356(6)	162
C19–H19B···I1	$-x+1, -y+1, -z+1$	0.95	3.26	4.164	154
C24–H24···I2	$-x, -y+2, -z+1$	0.98	3.21	3.900	131
C17–H17···I1	$1+x, y, z$	0.95	3.00	3.725(5)	134
C26–H26B···O1	$-1+x, y, 1+z$	0.98	2.56	3.538(7)	173
C26–H26C···I2	$-1+x, y, 1+z$	0.98	3.03	3.984(6)	166

Table 2. Main parameters of C–H···π contacts in the crystal of complex **1** (Cg_i is the centroid of the corresponding six-membered ring; H–Perp is the perpendicular distance from H to the ring plane; γ is the angle between the C–Cg_i vector and the normal to the ring plane).

C–H···Cg_i	Symmetry Operation	H···Cg, Å	H–Perp, Å	γ, °	C–H···Cg, °	C···Cg, Å
C6–H6···Cg_6(C13–C18)	–	2.59	2.51	14.88	143	3.402(4)
C15–H15···Cg_5(C4–C9)	$1-x, 1-y, 1-z$	2.79	2.72	12.29	144	3.598(5)
C19–H19A···Cg_4(C3C4C9–C12)	$1-x, 1-y, 1-z$	2.93	2.92	4.53	135	3.695(6)
C26–H26A···Cg_7(C20–C25)	$-x, 2-y, 2-z$	2.82	2.75	12.87	162	3.764(7)

The experimental powder X-ray diffraction pattern of the bulk sample is in good agreement with that calculated from the single-crystal X-ray diffraction data, confirming that complex **1** represents the predominant crystalline phase of the isolated material (Figure S3).

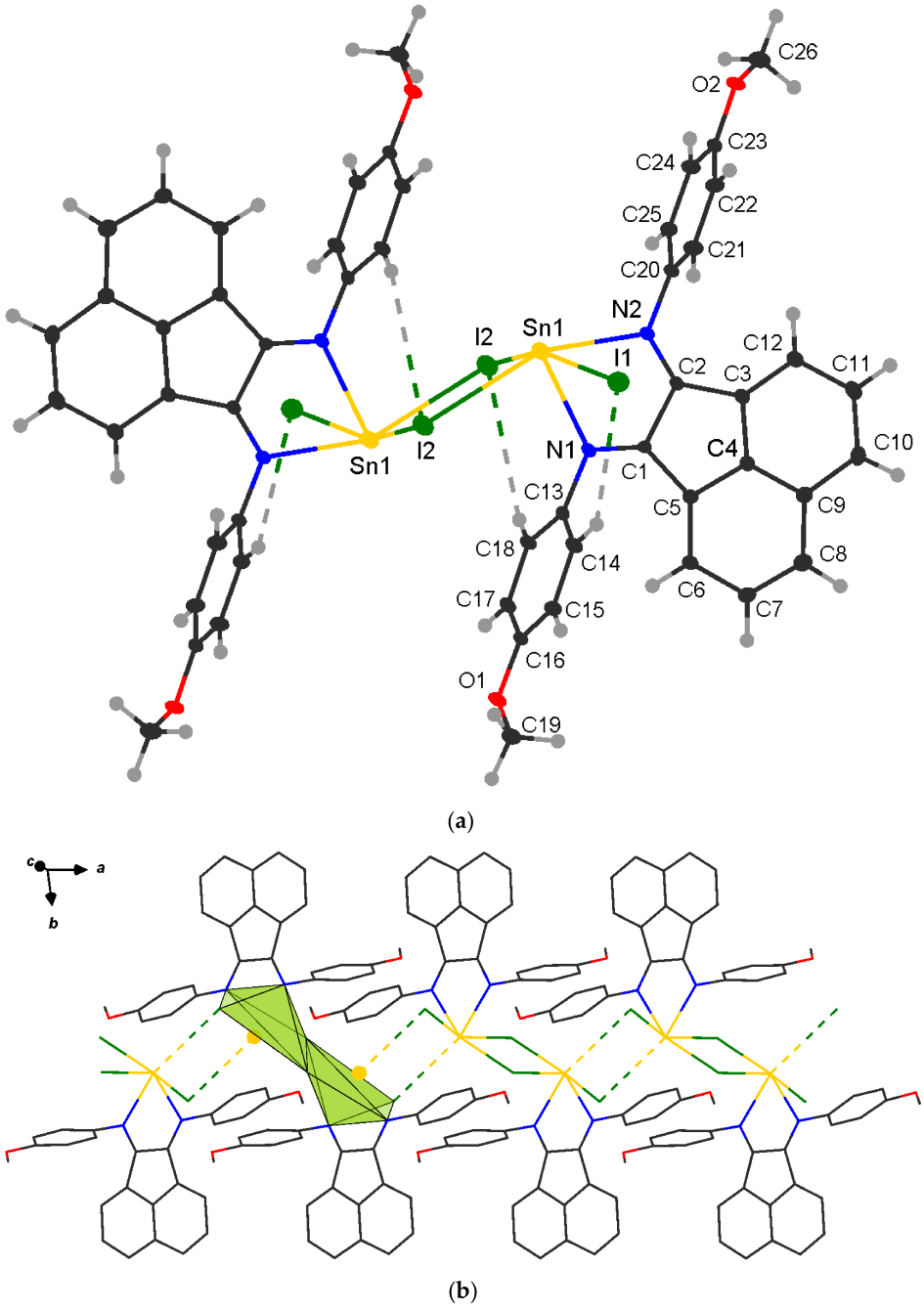


Figure 1. Molecular structure of complex **1** ((**a**), ellipsoids at 30% probability; intramolecular C–H···I contacts are shown by dashed line); fragment of the crystal packing and geometry of coordination polyhedron SnN_2I_3 ((**b**), hydrogen atoms are omitted; intramolecular Sn1···I1 contacts are shown as dashed lines).

2.3. Electrochemical Studies

The electrochemical behavior of complex **1** was studied by cyclic voltammetry (CV) in dichloromethane at a glassy carbon electrode (Figure 2).

For complex **1**, two quasi-reversible reduction peaks are observed at $E^{red1}_{1/2} = -1.26$ V and $E^{red12}_{1/2} = -1.73$ V. The current ratios for the first and second cathodic steps are 0.65 and 0.62, respectively, indicating a relative stability of the electrogenerated intermediates. The electron transfer is followed by a fast chemical step, which leads to a decrease in the current ratio and the appearance of a re-oxidation peak of the product of the chemical step at 0.65 V on the reverse scan of the voltammogram. The observed CV peaks can be

attributed to the formation of mono- and dianionic complexes containing the one- and two-electron reduced forms of the redox-active ligand (Scheme 3, **1** as monomer for clarity).

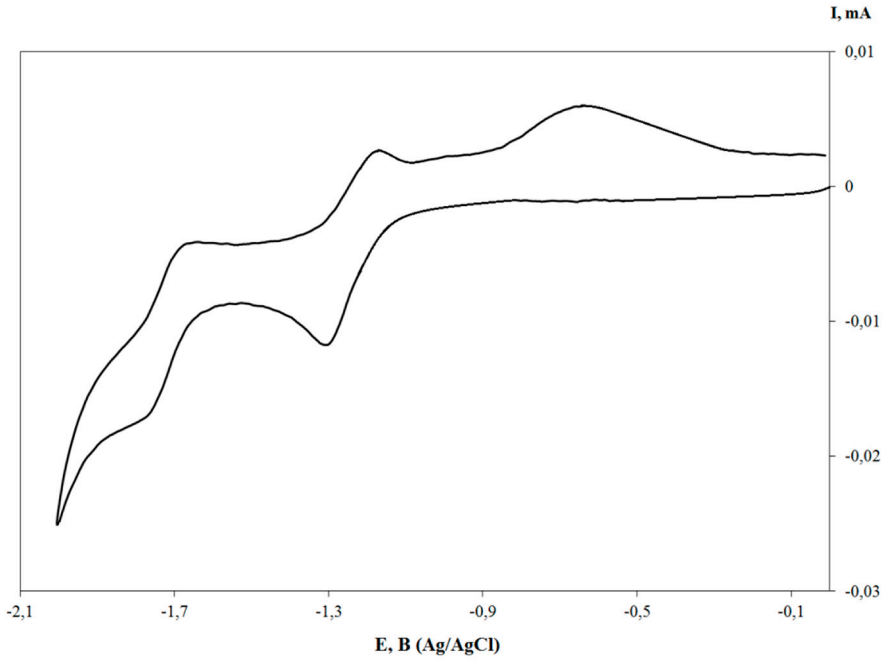
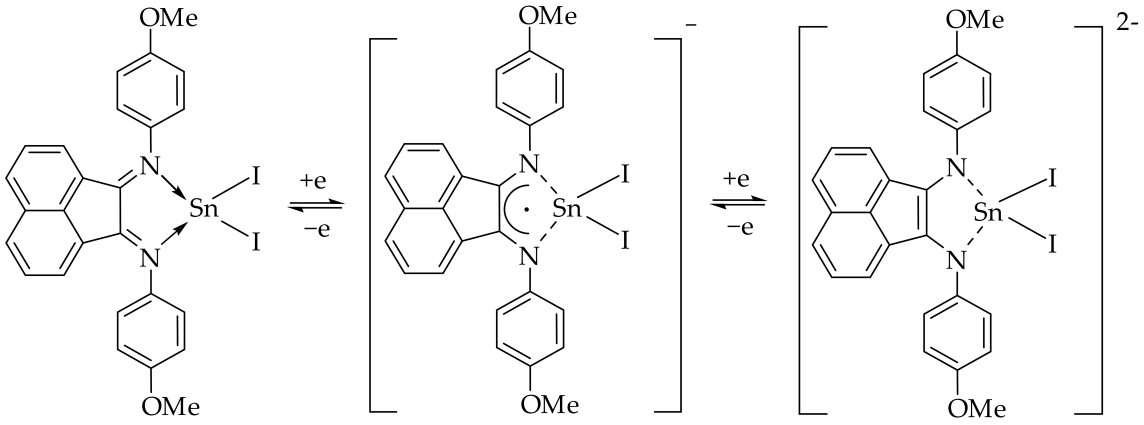


Figure 2. The CV reduction curve of complex **1** was recorded in the potential range from 0.0 to −2.0 V (CH_2Cl_2, glassy carbon electrode, C(I) = 0.0015 M, 0.15 M nBu_4NClO_4, scan rate 0.2 V/s, Ag/AgCl/KCl).



Scheme 3. Reduction of complex **1** with the formation of the mono- and dianionic species.

In contrast to the previously studied zinc(II) complexes with redox-active ligands [41–43], the interaction of the BIAN ligand with tin(II) iodide, which is a weak Lewis acid, results in a slight anodic shift in the reduction potentials of the redox-active ligand by 0.07–0.08 V compared to the free BIAN (Figure 3).

Under similar experimental conditions, the ligand undergoes electroreduction in two quasi-reversible one-electron steps at $E^{red1}{}_{1/2}$ = −1.34 V and $E^{red12}{}_{1/2}$ = −1.80 V. The current ratios are 0.44 and 0.78 for the first and second redox transitions, respectively. For the free BIAN ligand, the reverse scan of the CV curves shows re-oxidation peaks at −0.85 and −0.65 V. The electrogenerated mono- and dianionic forms exhibit increased basicity and are capable of protonation. The re-oxidation peak observed in the CV of complex **1** at −0.65 V can be attributed to the product of decoordination of the doubly reduced protonated form of the ligand. In the anodic region, an irreversible oxidation

peak is observed for complex **1** at 0.93 V, presumably corresponding to the oxidation of the Sn–I bond. A similar peak at 0.73–0.86 V was previously reported for zinc iodide and its complexes with redox-active ligands.

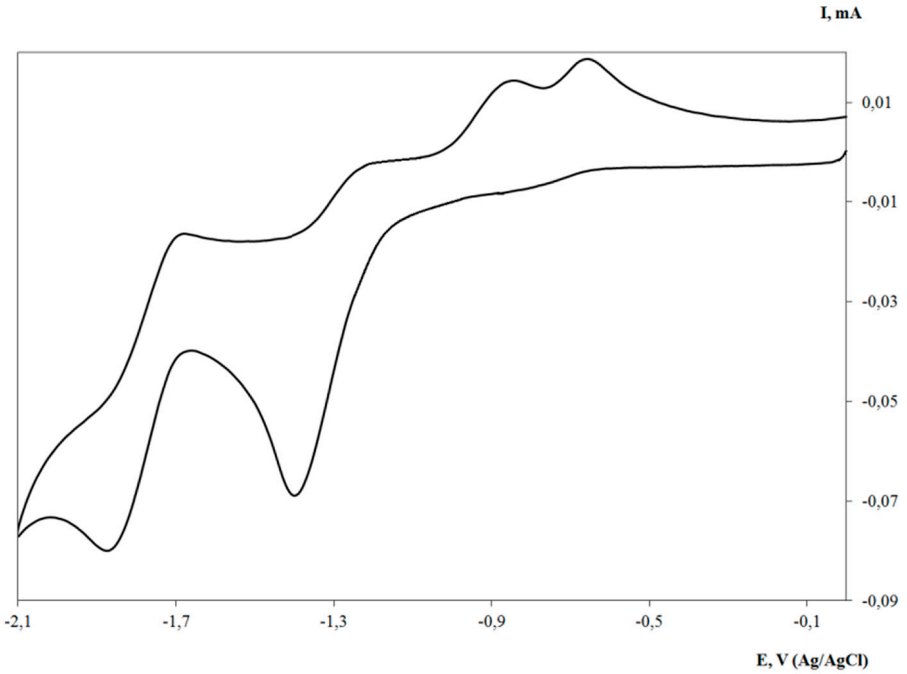


Figure 3. The CV reduction curve of free BIAN was recorded in the potential range from 0.0 to −2.1 V (CH_2Cl_2, glassy carbon electrode, C(I) = 0.0035 M, 0.15 M nBu_4NClO_4, scan rate 0.2 V/s, Ag/AgCl/KCl).

2.4. Antibacterial Activity

The antibacterial activity of the synthesized complex **1**, the related compound 4-MeO-MIAN, and the starting SnI_2 was evaluated against clinically significant strains of Gram-positive and Gram-negative bacteria (Tables 3 and 4). The parent tin salt exhibited pronounced bacteriostatic activity against *S. aureus* and *E. faecalis* ATCC 51299, with MIC values ranging from 40 to 62.5 μg/mL. At the same time, low antibacterial activity was observed for the strains *E. faecium* 1165, *E. faecium* 3994, and *E. faecalis* 3576. For the first five strains, the MIC values of complex **1** are comparable to those of the parent tin salt. Selectivity of action was noted for the strains *S. aureus* O1 and R1 (clinical isolates resistant to meropenem), as well as *E. faecium* 1165 and *E. faecalis* 3576 (78 μg/mL), surpassing the data for meropenem. The antibacterial activity of complex **1** is comparable to that of SnI_2 for several of the tested strains, while differences are observed for some clinical isolates. Since the antibacterial activity of free 4-MeO-BIAN was not determined in the present study, the individual contribution of the coordinated BIAN ligand to the activity of complex **1** cannot be unambiguously assessed.

The initial tin salt, complex **1**, and 4-MeO-MIAN do not exhibit pronounced antibacterial activity against the Gram-negative bacterium *E. coli* ATCC 25922: the MIC values ranged from 156 to 312.5 μg/mL.

Comparison of the minimum inhibitory concentration (MIC) and minimum bactericidal concentration (MBC) for the studied compounds reveals activity against Gram-positive cocci. All three compounds exhibit moderate antibacterial activity against *S. aureus* strains (including GISA) and enterococci. The MBC/MIC ratio is a characteristic of the type of action of a substance. For meropenem, the MBC equals the MIC in all cases, confirming its bactericidal effect. For the studied compounds, the MBC/MIC ratio in most cases

ranges from 1 to 5, which allows them to be classified as predominantly bactericidal agents, although less pronounced than meropenem. In the case of SnI_2, for staphylococci and some enterococci (e.g., *E. faecalis* 3576), the MBC/MIC ratio is 2, indicating bactericidal action. However, for *E. faecium* ATCC 29212 and strains 1165 and 3994, this ratio increases to 5–7.8, meaning that the effect becomes bacteriostatic at the MIC, and cell death occurs only at concentrations 5–8 times higher than the MIC. For *E. coli*, the MBC of SnI_2 is 625 μg/mL (MIC 156, ratio 4), indicating very weak bactericidal activity against this Gram-negative bacterium. The effect of the 4-MeO-MIAN ligand on bacteria is more diverse. Against *S. aureus* GISA and strain R1, the MBC/MIC ratio is 5 (bacteriostatic profile), while against *E. faecium* ATCC 29212 and *E. faecium* 1165, this parameter indicates bactericidal action with a ratio of 1.6–2. Against *E. coli*, with MBC = 312.5 μg/mL, the compound is moderately bactericidal.

Table 3. Minimum inhibitory concentration (MIC) of the compounds, μg/mL.

Strain	SnI_2	4-MeO-MIAN	Complex 1	Meropenem
S. aureus GISA ATCC 700699	62.5	62.5	**62.5**	32
S. aureus O1	40	78	**40**	32
S. aureus R1	78	78	**40**	32
E. faecium ATCC 29212	40	40	**40**	4
E. faecalis ATCC 51299	62.5	62.5	**62.5**	256
E. faecium 1165	156	31.2	**78**	128
E. faecium 3994	156	62.5	**156**	16
E. faecalis 3576	156	156	**78**	256
E. coli ATCC 25922	156	156	**312.5**	–

Table 4. Minimum bactericidal concentration (MBC) of the compounds, μg/mL.

Strain	SnI_2	4-MeO-MIAN	Complex 1	Meropenem
S. aureus GISA ATCC 700699	62.5	312.5	**156.3**	32
S. aureus O1	78	156.3	**78**	32
S. aureus R1	78	312.5	**156**	32
E. faecium ATCC 29212	312.5	62.5	**62.5**	4
E. faecalis ATCC 51299	62.5	62.5	**62.5**	256
E. faecium 1165	312.5	62.5	**312.5**	128
E. faecium 3994	312.5	312.5	**156**	16
E. faecalis 3576	312.5	312.5	**156.3**	256
E. coli ATCC 25922	625	312.5	**>625**	–

Complex **1** exhibits the most stable bactericidal profile. For most strains (all three *S. aureus* strains, *E. faecalis* ATCC 51299, *E. faecium* 3994, and *E. faecalis* 3576), the MBC/MIC ratio is 1–2, meaning that the bactericidal effect is achieved already at a concentration equal to or twice the MIC. Exceptions are *E. faecium* ATCC 29212 and *E. faecium* 1165, for which the bactericidal effect is noticeably weaker. Against *E. coli*, complex **1** is almost inactive, indicating a complete absence of bactericidal activity against Gram-negative microflora in the concentration range studied. The inefficacy against *E. coli* is typical for substances with low ability to penetrate the outer membrane of Gram-negative bacteria, which is associated

with the presence of an additional outer membrane that hinders the penetration of the complex into the cell.

The predominance of MBC values exceeding the MIC by no more than 4 times indicates that the studied compounds are not purely bacteriostatic agents but are capable of causing cell death at concentrations close to the inhibitory ones. Complex **1** is distinguished by its bactericidal activity, which is achieved already at the MIC (for many strains) or at a twofold excess.

In summary, the studied compounds exhibit moderate but stable activity against Gram-positive cocci, including strains with reduced susceptibility to meropenem. Based on the MBC/MIC ratio, they range from strictly bactericidal (complex **1**) to moderately bacteriostatic (in certain cases for SnI_2 and 4-MeO-MIAN). The most predictable bactericidal effect is demonstrated by compound **1**, which combines a redox-active ligand and a tin atom.

Further studies including direct comparison with the corresponding free BIAN ligand are required to clarify the effect of complex formation on the antibacterial activity.

It should be noted that complex **1** and SnI_2 exhibit identical or similar MIC values against several of the tested strains. The stability and speciation of complex **1** under the conditions of the antibacterial assays have not been investigated in the present study. Therefore, partial dissociation, hydrolysis, or other transformations of the complex in the culture medium cannot be excluded, and the observed antibacterial activity cannot be unequivocally attributed to the intact coordination complex. Further solution-stability and speciation studies under physiologically relevant conditions are required to clarify the nature of the biologically active species.

3. Materials and Methods

3.1. General Remarks

The synthesis of compound **1** was carried out using a modified Schlenk technique. Photographs of the main synthesis stages are available in the Supplementary Materials (Figure S2). Tetrahydrofuran (pure grade, "Khimmed") was dried by refluxing over sodium with benzophenone until a blue color appeared, then distilled and stored over sodium with benzophenone; it was condensed immediately prior to synthesis. Tin(II) iodide was synthesized in situ from elemental tin and iodine in tetrahydrofuran in a glass ampoule with a Teflon stopcock under heating. The diimine ligand (4-MeO-BIAN) and its monoimino derivative (4-MeO-MIAN) were obtained according to previously reported procedures [40,44].

IR spectra were recorded in the range of 400–4000 cm^{-1} on a Perkin Elmer Spectrum 65 spectrophotometer (Waltham, MA, USA) equipped with a Quest ATR Accessory (Specac, Orpington, UK) using the attenuated total reflection (ATR) technique. Elemental analysis was performed on an automatic CHNS analyzer EuroEA-3000 (EuroVektor, Pavia, Italy).

Single-crystal X-ray diffraction data of **1** were collected on a Bruker D8 Venture diffractometer equipped with a two-dimensional CCD detector using MoKα radiation (λ = 0.71073 Å) and a graphite monochromator. Absorption was corrected empirically using the SADABS program [45]. The structure was solved using SHELXT [46] incorporated in the OLEX^2 1.5 program package [47]. All non-hydrogen atoms were located from difference Fourier maps and refined anisotropically against F^2_{hkl} using SHELXL 2018/3 [46]. Hydrogen atoms on carbon atoms of the organic ligands were generated geometrically and refined using a riding model. Crystallographic data, experimental parameters at T = 100(2) K, and refinement details are as follows: CCDC No. 2584822, formula $C_{26}H_{20}I_2N_2O_2Sn$, M = 764.93 g mol^{-1}, triclinic space group *P*–1, a = 9.1383(5) Å, b = 12.1567(5) Å, c = 13.4549(7) Å, α = 64.274(2)°, β = 78.066(2)°, γ = 69.895(2)°, V = 1261.58(11) Å^3, Z = 2, T_{min}/T_{max} = 0.4663/0.7467,

μ = 3.485 mm^{-1}, d_{calc} = 2.014 g cm^{-3}, θ_{max} = 34.02°, R_{int} = 0.0274, 14,356 measured reflections, 8391 independent reflections, 7694 reflections with $I > 2\sigma(I)$, *GooF* = 1.153, $R_1(I > 2\sigma(I))$ = 0.0536, $wR_2(I > 2\sigma(I))$ = 0.1552, R_1(all) = 0.0562, wR_2(all) = 0.1577, ρ_{min}/ρ_{max} = −3.180/1.952 e Å^{-3}.

Powder X-ray diffraction data for compound **1** were obtained at 20 °C on a Bruker D8 Advance diffractometer (CuKα, λ = 1.54060 Å, Ni filter, reflection geometry, LynxEye detector). The measurement was performed in the 2θ range of 5–50° with a step of 0.020°. The sample was finely dispersed on a zero-background silicon holder. Rietveld refinement was carried out using TOPAS 4 software [48]. The structure of compound **1** determined by single-crystal X-ray diffraction at low temperature was used as the initial model.

Electrochemical measurements were performed by cyclic voltammetry (CV) using an IPC-pro potentiostat (Russia, LLC STF "Volta", St. Petersburg, Russia) in a three-electrode cell under an argon atmosphere in dichloromethane. A stationary glassy carbon (GC) electrode with a diameter of 2 mm served as the working electrode, and a platinum plate (S = 18 mm^2) was used as the auxiliary electrode. The reference electrode was Ag/AgCl/KCl with a waterproof diaphragm. The scan rate was 0.2 V s^{-1}. Tetrabutylammonium perchlorate (0.15 M n-Bu_4NClO_4) was used as the supporting electrolyte.

The antibacterial activity of the synthesized complex **1**, the related compound 4-MeO-MIAN, and the starting SnI_2 was studied by the microdilution method in plates against clinically significant strains of Gram-positive and Gram-negative bacteria. The test cultures included reference and clinical strains of *Staphylococcus aureus*, *Enterococcus faecium*, *Enterococcus faecalis*, and *Escherichia coli*. Meropenem was used as the reference antibiotic. Stock solutions of the compounds were prepared in DMSO at a concentration of 5000 μg/mL (500 μg/mL for repeated experiments). The minimum inhibitory concentration (MIC) was determined after 20–24 h of incubation, and the minimum bactericidal concentration (MBC) was determined after 48 h. The MIC and MBC assays were performed in triplicate in two independent experiments. The obtained endpoint values were identical across the replicate measurements; therefore, the corresponding standard deviation was zero.

Antibacterial activity was assessed against bacterial strains *S. aureus* ATCC 29213, *S. aureus* ATCC 6538P, and *E. coli* ATCC 25922 obtained from the American Type Culture Collection (ATCC, Manassas, VA, USA). The minimum inhibitory concentration (MIC, μg/mL) was determined by the broth microdilution method in Mueller–Hinton broth (MHB) according to the Clinical and Laboratory Standards Institute (CLSI) guidelines [49]. The test compounds were dissolved in dimethyl sulfoxide (DMSO) at an initial concentration of 5000 μg/mL (500 μg/mL for repeated experiments), diluted with MHB, and tested in a concentration range from 312.50 to 0.61 μg/mL. The final DMSO concentration was below 12.5% and did not affect microbial growth. Inoculates were adjusted to approximately 5 × 10^5 CFU/mL. The diluted bacterial cultures in MHB were incubated at 37 °C for 24 h. MIC values were determined visually as the lowest concentration of the test compound resulting in complete inhibition of growth. The minimum bactericidal concentration (MBC) was determined after 48 h. Each assay was performed in triplicate in two independent experiments. DMSO at a concentration of 12.5% was used as a negative control, and meropenem was used as a positive control.

*3.2. Synthesis of [(4-MeO-BIAN)SnI(μ-I)]$_2$ (**1**)*

Tin(II) iodide was prepared in situ by the reaction of elemental tin with iodine in anhydrous THF. A detailed synthetic procedure and characterization of the obtained SnI_2 by powder X-ray diffraction are provided in the Supporting Information (Figure S4).

Method A. A solution of SnI_2 in THF (0.5 mmol in 15 mL) was prepared in a separate glass ampoule with a Teflon stopcock and transferred into a glass ampoule with a magnetic

stir bar. In another glass ampoule, a sample of 4-MeO-BIAN (0.1963 g, 0.5 mmol) was placed and degassed under dynamic vacuum for 20 min. Anhydrous THF (5 mL) was condensed into the ampoule with the ligand, and the resulting solution was then poured into the ampoule with the SnI_2. The latter was sealed and left to stir at room temperature for 3 h (the color of the reaction mixture was brown). Stirring of the reaction mixture led to the formation of dark red crystals of compound (**1**). The yield was 0.321 g (84%).

Method B. A solution of SnI_2 in THF (0.5 mmol in 15 mL) was prepared in a separate glass ampoule with a Teflon stopcock and transferred into a glass ampoule. In another glass ampoule, a weight amount of 4-MeO-MIAN (0.1437 g, 0.5 mmol) was placed and degassed under dynamic vacuum for 20 min. Anhydrous THF (5 mL) was condensed into the ampoule with the ligand, and the resulting solution was then poured into the ampoule with the SnI_2. The latter was sealed and heated in an oil bath at 80 °C for 3 h. Heating of the reaction mixture led to the formation of dark red crystals of compound (**1**). The yield was 0.119 g (31%).

Elemental analysis calculated for $C_{26}H_{20}I_2N_2O_2Sn$ (%): C, 40.83; H, 2.64; N, 3.66. Found (%): C, 39.77; H, 2.88; N, 3.76.

IR spectrum (ATR; ν, cm^{-1}): 3902 w, 3873 w, 3853 w, 3838 w, 3818 w, 3801 w, 3748 w, 3734 w, 3705 w, 3674 w, 3649 w, 3612 w, 3561 w, 2962 w, 2902 w, 2830 w, 1697 w, 1650 w, 1596 w, 1577 w, 1499 m, 1460 w, 1433 w, 1415 w, 1290 w, 1242 s, 1178 m, 1164 m, 1096 s, 1018 vs, 944 w, 853 w, 825 s, 798 vs, 775 s, 716 m, 689 w, 650 w, 594 m, 547 m.

^{1}H NMR (300 MHz, DMSO-*d6*) δ, ppm: 8.09 (d, 2H, C(5)H, J = 8.2 Hz), 7.54 (t, 2H, C(4)H, J = 7.6 Hz), 7.11–7.03 (m, 8H, C_6H_4), 6.93 (d, 2H, C(3)H, J = 7.2 Hz), 3.83 (s, 6H, OMe).

4. Conclusions

Thus, a new tin(II) complex with the redox-active ligand 4-MeO-BIAN has been synthesized and characterized by single-crystal X-ray diffraction, IR spectroscopy, elemental analysis, and powder X-ray diffraction. It was also found that the molecular complex can be formed in the reaction of SnI_2 with 4-MeO-MIAN as a result of rearrangement at the metal center into the corresponding symmetrical ligand BIAN, but with a lower yield. Based on the obtained structural data, it has been demonstrated that the reaction product represents a binuclear molecule featuring two bridging iodide anions and chelate-bound ligands in their neutral form. Intermolecular Sn···I interactions give rise to the formation of a one-dimensional supramolecular chain. Cyclic voltammetry revealed that the reduction of complex **1** in CH_2Cl_2 proceeds in two consecutive quasi-reversible steps, corresponding to the formation of the mono- and dianionic forms of the complex containing the radical-anionic and doubly reduced forms of the redox-active ligand. Coordination of the α-diimine ligand to tin(II) iodide, acting as a weak Lewis acid, results in an anodic shift in the redox transitions by 0.07–0.08 V compared to the free BIAN ligand, indicating a weak influence of the metal center on the redox properties of the ligand. Complex **1** was shown to exhibit antibacterial activity in vitro against clinically significant strains of Gram-positive bacteria, which opens up prospects for further investigation of its biological properties.

Supplementary Materials: The following supporting information can be downloaded at https://www.mdpi.com/article/10.3390/molecules31203676/s1, Figure S1: IR-Spectra of **1** (solid sample, RT, attenuated total reflection technique); Figure S2: Step-by-step synthesis of complex **1**; Figure S3: Experimental (blue curve) and calculated (red curve) powder diffraction patterns for compound **1** and their difference (grey curve); Figure S4: Step-by-step synthetic operations of SnI_2 preparation; Figure S5: Experimental (blue curve) and calculated (red curve) powder X-ray diffraction patterns of SnI_2 and their difference (grey curve); Figure S6. ^{1}H NMR of [(4-MeO-BIAN)SnI(μ-I)]$_2$ (300 MHz, DMSO-d6).

Author Contributions: Conceptualization, D.S.Y. and A.A.T.; synthesis and characterization, A.A.T.; cyclic voltammetry and antibacterial activity evaluation, I.V.S.; powder X-ray diffraction analysis, N.V.G.; ligand synthesis, A.N.L.; single-crystal X-ray diffraction analysis, M.A.K.; manuscript writing, A.A.T., D.S.Y., and M.A.K.; funding acquisition, D.S.Y. All authors have read and agreed to the published version of the manuscript.

Funding: This work was supported by the Ministry of Science and Higher Education of the Russian Federation as part of the State Assignment of the Kurnakov Institute of General and Inorganic Chemistry of the Russian Academy of Sciences.

Institutional Review Board Statement: Not applicable.

Informed Consent Statement: Not applicable.

Data Availability Statement: The structure parameters of the obtained compound were deposited with the Cambridge Structural Database (CCDC 2584822) deposit@ccdc.cam.ac.uk or http://www.ccdc.cam.ac.uk/data_request/cif (accessed on 3 September 2026).

Acknowledgments: The authors express their gratitude to the JRC PMR IGIC RAS for the opportunity to carry out research using the center's equipment.

Conflicts of Interest: The authors declare no conflicts of interest. The funders had no role in the design of the study; in the collection, analyses, or interpretation of data; in the writing of the manuscript; or in the decision to publish the results.

References

1. Kaim, W. The Shrinking World of Innocent Ligands: Conventional and Non-Conventional Redox-Active Ligands. *Eur. J. Inorg. Chem.* **2012**, *2012*, 343–348. [CrossRef]
2. De Bruin, B.; Hetterscheid, D.G.H.; Koekkoek, A.J.J.; Grützmacher, H. The Organometallic Chemistry of Rh-, Ir-, Pd-, and Pt-Based Radicals: Higher Valent Species. In *Progress in Inorganic Chemistry*; Karlin, K.D., Ed.; Wiley: Hoboken, NJ, USA, 2007; Volume 55, pp. 247–354.
3. Kaim, W.; Schwederski, B. Non-Innocent Ligands in Bioinorganic Chemistry—An Overview. *Coord. Chem. Rev.* **2010**, *254*, 1580–1588. [CrossRef]
4. Fan, Y.; Jiang, B.; Zhang, Z.; Zhang, H.; Yang, L.; Chen, T.; He, L.; Liu, Y.; Guo, J.; Zhao, T.; et al. Packing Order Control in Conductive Metal–Organic Frameworks by Tuning Ligand Oxidation State. *Angew. Chem. Int. Ed.* **2026**, *65*, e202522424. [CrossRef] [PubMed]
5. Hasegawa, G.; Yano, M.; Miyanishi, M.; Shiota, Y.; Yoshizawa, K.; Itoh, S.; Sugimoto, H. Redox Characteristics of a Lead(II) Complex Supported by a o-Phenylenediamido Ligand. *Bull. Chem. Soc. Jpn.* **2026**, *99*, uoag018. [CrossRef]
6. King, L.O.; Gullett, K.L.; Mitchell, A.W.; Coughlin, E.J.; Zeller, M.; Bart, S.C. Amidophenolate Lanthanide Complexes and Their Multielectron Reactivity. *Inorg. Chem.* **2026**, *65*, 7781–7788. [CrossRef] [PubMed]
7. Vala, S.; Krisch, D.; Pilz, D.; Offenthaler, S.; Schöfberger, W. Catalyst Identity Matters: Molecular Ag(I)–BIAN Complexes Outperform Ag Nanoparticles in High-Current CO_2 Electroreduction. *ACS Omega* **2026**, *11*, 53833–53842. [CrossRef] [PubMed]
8. Chirik, P.J. Preface: Forum on Redox-Active Ligands. *Inorg. Chem.* **2011**, *50*, 9737–9740. [CrossRef] [PubMed]
9. Anthony, E.J.; Bolitho, E.M.; Bridgewater, H.E.; Carter, O.W.L.; Donnelly, J.M.; Imberti, C.; Lant, E.C.; Lermyte, F.; Needham, R.J.; Palau, M.; et al. Metallodrugs Are Unique: Opportunities and Challenges of Discovery and Development. *Chem. Sci.* **2020**, *11*, 12888–12917. [CrossRef] [PubMed]
10. Mjos, K.D.; Orvig, C. Metallodrugs in Medicinal Inorganic Chemistry. *Chem. Rev.* **2014**, *114*, 4540–4563. [CrossRef] [PubMed]
11. Zhang, P.; Sadler, P.J. Redox-Active Metal Complexes for Anticancer Therapy. *Eur. J. Inorg. Chem.* **2017**, *2017*, 1541–1548. [CrossRef]
12. Baryshnikova, S.V.; Poddel'sky, A.I. Heteroligand Metal Complexes with Extended Redox Properties Based on Redox-Active Chelating Ligands of o-Quinone Type and Ferrocene. *Molecules* **2022**, *27*, 3928. [CrossRef] [PubMed]
13. Fomenko, I.S.; Romashev, N.F.; Gushchin, A.L. Advances in the Chemistry of Redox-Active Bis(Imino)Acenaphthenes (BIAN): A Case of Transition Metal Complexes. *Coord. Chem. Rev.* **2024**, *514*, 215845. [CrossRef]
14. Mukherjee, N.; Majumdar, M. Ligand-Centered Redox-Assisted Synthesis of a Bis(imino)acenaphthene-Stabilized Tellurium(II) Dicationic Compound. *Organometallics* **2026**, *45*, 637–640. [CrossRef]

15. Skatova, A.A.; Bazanov, A.A.; Baranov, E.V.; Kiskin, M.A.; Ketkov, S.Y.; Fedushkin, I.L. Gallium phosphaketenes derived from bis(imino)acenaphthenes (bian): Synthesis and reactivity towards a trityl radical and bian-gallylene. *Dalton Trans.* **2026**, *55*, 2080–2087. [CrossRef] [PubMed]
16. Khrizanforova, V.V.; Fayzullin, R.R.; Krasovskaya, E.B.; Agarkov, A.S.; Mingazhetdinova, D.O.; Gerasimova, T.P.; Morozov, V.I.; Budnikova, Y.H. New acenaphthene-based heterocycles: Synthesis, crystal structure, and spectroelectrochemistry. *Struct. Chem.* **2026**, *37*, 2481–2490. [CrossRef]
17. Romashev, N.F.; Abramov, P.A.; Bakaev, I.V.; Fomenko, I.S.; Samsonenko, D.G.; Novikov, A.S.; Tong, K.K.H.; Ahn, D.; Dorovatovskii, P.V.; Zubavichus, Y.V.; et al. Heteroleptic Pd(II) and Pt(II) Complexes with Redox-Active Ligands: Synthesis, Structure, and Multimodal Anticancer Mechanism. *Inorg. Chem.* **2022**, *61*, 2105–2118. [CrossRef] [PubMed]
18. Gushchin, A.L.; Romashev, N.F.; Shmakova, A.A.; Abramov, P.A.; Ryzhikov, M.R.; Fomenko, I.S.; Sokolov, M.N. Novel Redox Active Rhodium(III) Complex with Bis(Arylimino)Acenaphthene Ligand: Synthesis, Structure and Electrochemical Studies. *Mendeleev Commun.* **2020**, *30*, 81–83. [CrossRef]
19. Romashev, N.F.; Gushchin, A.L.; Fomenko, I.S.; Abramov, P.A.; Mirzaeva, I.V.; Kompan'kov, N.B.; Kal'nyi, D.B.; Sokolov, M.N. A New Organometallic Rhodium(I) Complex with Dpp-Bian Ligand: Synthesis, Structure and Redox Behaviour. *Polyhedron* **2019**, *173*, 114110. [CrossRef]
20. Wu, C.; Romashev, N.F.; Komlyagina, V.I.; Petrović, T.; Bakaev, I.V.; Abramov, P.A.; Wang, Y.; Ryadun, A.A.; Fomenko, I.S.; Zou, T.; et al. Immunogenic cell death-inducing Rh(i) and Ir(i) complexes with bis(imino)acenaphthene-derived ligands: Insights into the role of the metal center and the ligands. *Inorg. Chem. Front.* **2026**, *13*, 403–419. [CrossRef]
21. Lukoyanov, A.N.; Fomenko, I.S.; Gongola, M.I.; Shul'pina, L.S.; Ikonnikov, N.S.; Shul'pin, G.B.; Ketkov, S.Y.; Fukin, G.K.; Rumyantcev, R.V.; Novikov, A.S.; et al. Novel Oxidovanadium Complexes with Redox-Active R-Mian and R-Bian Ligands: Synthesis, Structure, Redox and Catalytic Properties. *Molecules* **2021**, *26*, 5706. [CrossRef] [PubMed]
22. Fomenko, I.S.; Koshcheeva, O.S.; Kuznetsova, N.I.; Larina, T.V.; Gongola, M.I.; Afewerki, M.; Abramov, P.A.; Novikov, A.S.; Gushchin, A.L. Novel Copper(II) Complexes with BIAN Ligands: Synthesis, Structure and Catalytic Properties of the Oxidation of Isopropylbenzene. *Catalysts* **2023**, *13*, 849. [CrossRef]
23. Komlyagina, V.I.; Romashev, N.F.; Besprozvannykh, V.K.; Arakelyan, J.; Wu, C.; Chubarov, A.S.; Bakaev, I.V.; Soh, Y.K.; Abramov, P.A.; Cheung, K.L.; et al. Effects of Bis(Imino)Acenaphthene (Bian)-Derived Ligands on the Cytotoxicity, DNA Interactions, and Redox Activity of Palladium(II) Bipyridine Complexes. *Inorg. Chem.* **2023**, *62*, 11541–11553. [CrossRef] [PubMed]
24. Bakaev, I.V.; Romashev, N.F.; Komlyagina, V.I.; Samsonenko, D.G.; Gushchin, A.L. Mono(Arylhydrazino)Acenaphthenones as a Platform for the Design of NIR Chromophores Based on Pd(II)-BIAN Complexes. *New J. Chem.* **2023**, *47*, 18825–18834. [CrossRef]
25. Bardina, E.E.; Shmelev, N.Y.; Albrekht, Y.N.; Koon, W.K.Y.; Abramov, P.A.; Mirzaeva, I.V.; Sheven, D.G.; Makotchenko, E.V.; Fomenko, I.S.; Lukoyanov, A.N.; et al. Gold(I) Complexes with Redox Active BIAN and MIAN Ligands: Synthesis, Structure and Electrochemistry. *New J. Chem.* **2023**, *47*, 18251–18259. [CrossRef]
26. Singh, J.; Jaiswal, A.; Pal, A.K. Some Neoteric Tin Complexes Used in Biological Properties. *Am. J. Pharmacol. Sci.* **2023**, *11*, 21–27. [CrossRef]
27. Phor, A.; Mamta, B.; Subhash, M.; Phor, J.S.; Chaudhary, A. Potentially Biodynamic Tin(II) Complexes Derived from Macrocyclic Ligands: Synthesis, Spectral Analysis, In vitro Antibacterial, Antifungal and Brine Shrimp Lethality Evaluation. *Orient. J. Chem.* **2024**, *40*, 82–89. [CrossRef]
28. Neelofar, N.; Ali, N.; Ahmad, S.; El-Salam, N.M.A.; Ullah, R.; Nawaz, R.; Ahmad, S. Synthesis and Evaluation of Antioxidant and Antimicrobial Activities of Schiff Base Tin(II) Complexes. *Trop. J. Pharm. Res.* **2016**, *15*, 2693–2700. [CrossRef]
29. Bansal, N.; Dave, S. Synthesis, Spectral, Antimicrobial, and Antifertility Studies of Tetraaza Macrocyclic Complexes of Tin(II). *Main Group Met. Chem.* **2013**, *36*, 101–107. [CrossRef]
30. Stefanizzi, V.; Minutolo, A.; Molimbou, E.; Balestrieri, E.; Giudice, M.; Cordero, F.M.; Mosca, C.; Mastino, A.; Macchi, B.; Matteucci, C.; et al. Cytotoxic Effects of a Triorganotin Derivative on HTLV-1-Infected Cells at Different Immortalization/Transformation Stages In Vitro. *Molecules* **2026**, *31*, 349. [CrossRef] [PubMed]
31. Barwa, P.; Asija, S. Exploring hydrazone-derived organotin(IV) complexes as multifunctional antimicrobial and anticancer agents: A review. *Chem. Pap.* **2026**, *80*, 8533–8556. [CrossRef]
32. Das, S.; Pattanayak, P.D.; Sasamori, T.; Nakamura, T.; Dinda, R. Organotin(IV) Azo Hydrazonates as Lysosome-Targeted Imaging and Anticancer Agents. *Chem. Asian J.* **2026**, *21*, e00912. [CrossRef] [PubMed]
33. Kumar, M.; Abbas, Z.; Siwach, P.; Sharma, J.; Rani, A.; Sharma, S.; Aggarwal, P.; Show, P.; Haque, S.; Garg, V.; et al. Path of Organotin Complexes: Synthetic Factors, Mechanisms, and Broad Spectrum Biological Influences. *J. Adv. Biotechnol. Exp. Ther.* **2023**, *6*, 386. [CrossRef]
34. Subhashini, P.J.; Chandrabooma, P.; Gowri, M. Evaluation of the Anticancer Activity of Sulfonamides and Their Metal Complexes as Promising Therapeutic Agents. *Russ. J. Bioorg. Chem.* **2026**, *52*, 43. [CrossRef]

35. Singh, G.; Jyoti; Singh, A.; Gill, B.S.; Goyal, S.; Kaur, A. Integrating Sn(II) sensing with antioxidant and anticancer activities: Benzophenone appended triazole functionalized organosilane as a dual functional platform. *Inorg. Chem. Commun.* **2026**, *191*, 117003. [CrossRef]
36. Dodonov, V.A.; Kushnerova, O.A.; Rumyantsev, R.V.; Ulivanova, E.A.; Lukoyanov, A.N.; Razborov, D.A.; Fedyushkin, I.L. Tin Amides Based on Ligands of the Acenaphthene Imine Series. *Russ. J. Coord. Chem.* **2022**, *48*, 412–421. [CrossRef]
37. Piskunov, A.V.; Tsys, K.V.; Chegerev, M.G.; Cherkasov, A.V. Tin(II) Complexes Based on N-Alkyl-Substituted o-Amidophenolate Ligands: Acid–Base and Redox Transformations. *Russ. J. Coord. Chem.* **2019**, *45*, 626–636. [CrossRef]
38. Dodonov, V.A.; Kushnerova, O.A.; Razborov, D.A.; Baranov, E.V.; Ulivanova, E.A.; Lukoyanov, A.N.; Fedushkin, I.L. Stannylenes Based on Neutral, Anionic, and Dianionic 1,2-Bis[(2,6-Diisopropylphenyl)Imino]Acenaphthene. *Russ. Chem. Bull.* **2022**, *71*, 322–329. [CrossRef]
39. Lukoyanov, A.N.; Romashev, N.F.; Komlyagina, V.I.; Kokovkin, V.V.; Cherkasov, A.V.; Gushchin, A.L. Reactions of Palladium(II) Chloride with Monoiminoacenaphthenones. *Russ. J. Coord. Chem.* **2023**, *49*, 800–806. [CrossRef]
40. Yambulatov, D.S.; Nikolaevskii, S.A.; Lukoyanov, A.N.; Shmelev, M.A.; Voronina, J.K.; Babeshkin, K.A.; Matiukhina, A.K.; Efimov, N.N.; Kiskin, M.A.; Eremenko, I.L. A New Cobalt(II)–Lithium(I) Carboxylate Complex with an N,O-Donor Mono-Iminoacenaphthenone Ligand: Synthesis, Structure and Magnetic Behavior. *New J. Chem.* **2023**, *47*, 19362–19366. [CrossRef]
41. Poddel'sky, A.I.; Smolyaninov, I.V.; Druzhkov, N.O.; Fukin, G.K. Heterometallic Antimony(V)-Zinc and Antimony(V)-Copper Complexes Comprising Catecholate and Diazadiene as Redox Active Centers. *J. Organomet. Chem.* **2021**, *952*, 121994. [CrossRef]
42. Ershova, I.V.; Meshcheryakova, I.N.; Trofimova, O.Y.; Pashanova, K.I.; Arsenyeva, K.V.; Khamaletdinova, N.M.; Smolyaninov, I.V.; Arsenyev, M.V.; Cherkasov, A.V.; Piskunov, A.V. Complexes of Metal Halides with Unreduced O-(Imino)Quinones. *Inorg. Chem.* **2021**, *60*, 12309–12322. [CrossRef] [PubMed]
43. Yambulatov, D.S.; Gogoleva, N.V.; Smolyaninov, I.V.; Bushuev, V.A.; Tychinina, A.A.; Samulionis, A.S.; Voronina, J.K.; Skabitsky, I.V.; Shapovalov, S.S.; Nikolaevskii, S.A.; et al. Zinc(II) Iodide Complexes with Redox-Active α-Diimine Ligands: Synthesis, Structure, Spectroscopic and Electrochemical Properties. *Crystals* **2025**, *15*, 967. [CrossRef]
44. Gasperini, M.; Ragaini, F.; Cenini, S. Synthesis of Ar-BIAN Ligands (Ar-BIAN = Bis(Aryl)Acenaphthenequinonediimine) Having Strong Electron-Withdrawing Substituents on the Aryl Rings and Their Relative Coordination Strength toward Palladium(0) and -(II) Complexes. *Organometallics* **2002**, *21*, 2950–2957. [CrossRef]
45. Krause, L.; Herbst-Irmer, R.; Sheldrick, G.M.; Stalke, D. Comparison of Silver and Molybdenum Microfocus X-Ray Sources for Single-Crystal Structure Determination. *J. Appl. Crystallogr.* **2015**, *48*, 3–10. [CrossRef] [PubMed]
46. Sheldrick, G.M. SHELXT—Integrated Space-Group and Crystal-Structure Determination. *Acta Crystallogr. A Found. Adv.* **2015**, *71*, 3–8. [CrossRef] [PubMed]
47. Dolomanov, O.V.; Bourhis, L.J.; Gildea, R.J.; Howard, J.A.K.; Puschmann, H. OLEX2: A Complete Structure Solution, Refinement and Analysis Program. *J. Appl. Crystallogr.* **2009**, *42*, 339–341. [CrossRef]
48. Scarlett, N.V.Y.; Madsen, I.C. Quantification of Phases with Partial or No Known Crystal Structures. *Powder Diffr.* **2006**, *21*, 278–284. [CrossRef]
49. Smolyaninov, I.V.; Burmistrova, D.A.; Pomortseva, N.P.; Polovinkina, M.A.; Demidov, O.P.; Al'myasheva, N.R.; Poddel'skii, A.I.; Berberova, N.T. Triphenylphosphine Thiolate Gold(I) Complexes with Redox-Active Schiff Bases: Synthesis, Electrochemical Properties, and Biological Activity. *Russ. J. Coord. Chem.* **2023**, *49*, 577–592. [CrossRef]

Disclaimer/Publisher's Note: The statements, opinions and data contained in all publications are solely those of the individual author(s) and contributor(s) and not of MDPI and/or the editor(s). MDPI and/or the editor(s) disclaim responsibility for any injury to people or property resulting from any ideas, methods, instructions or products referred to in the content.